Study of $B^0 \to K^{*0}\tau\tau$ at FCC-*ee*

Tristan Miralles - FCC Clermont group

FCC Physics Workshop Annecy : 30^{th} of January

$b \to s\tau\tau$ and objectives

- Third generation couplings in quark transitions are the less-well known.
- Specific models addressing the Flavour problem(s) often provide $b \to \tau$ enhancements or modifications w.r.t. the SM $\Rightarrow b \to s\tau\tau$ ($m_\tau \sim 20 m_\mu$) is a must do to sort out the BSM models [1, 2]. Problem : measuring the ν's.
- Thanks to its clear experimental environment and its ability to produce boosted *b*-hadrons, FCC-*ee* looks like the right place to reconstruct the ν's.
- SM : the $b \to s\tau\tau$ transition proceeds through an electroweak penguin diagram.
- Study of the rare heavy-flavoured decay $B^0 \to K^*\tau^+\tau^-$ at FCC-*ee* [3]. SM prediction : BR=$\mathcal{O}(10^{-7})$ $\to$ not observed yet (present limit : $\mathcal{O}(10^{-3} - 10^{-4})$ [4]).

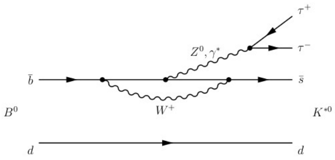

EW penguin quark-level transition

Topology

- The $B^0 \to K^*\tau\tau$ decay topology is driven by the tau decay multiplicity.
- There are from 2 to 4 neutrinos (not detected) and at least 4 charged particles in the final state and one, two or three decay vertices.
- We focus on the 3-prongs tau decays ($\tau \to \pi\pi\pi\nu$) for which the decay vertex can be reconstructed in order to solve fully the kinematics.
- 10 particles in the final state ($K, 7\pi, \nu, \bar{\nu}$), 3 decay vertices and 2 undetected neutrinos.

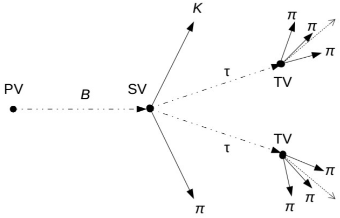

Decay topology

Goal : explore the feasibility of the search for $B^0 \to K^*\tau^+\tau^-$ and give the corresponding detector requirements.

Data and software used

- The events used in this work are generated with Pythia [5] ($Z \to b\bar{b}$ and hadronisation) and EvtGen [6] (forcing the decay with adequate models).
- The reconstruction is performed with the FCC Analyses sw using Delphes [7] simulation (featuring the IDEA [8] detector).
- The simulated data use particles reconstructed with the momentum resolution given by IDEA.
- The vertex resolutions drives the feasability of the measurement (Krakow) $\to$ the main goal of the study is to address the precision of the BF as function of the vertex resolution.
- State of the art IDEA vertexing performance will be determined and compared to other working points.

Reconstruction method

- To fully reconstruct the kinematics of the decay $\rightarrow$ neutrinos momenta must be resolved.
- Enough constraints are available to determine the missing coordinates.
- Energy momentum conservation at τ decay vertex $\Rightarrow$ gives the neutrino momentum at the cost of a quadratic ambiguity :

$$\begin{cases} p^{\perp}_{\nu_\tau} = -p^{\perp}_{\pi_t} \\ p^{\parallel}_{\nu_\tau} = \dfrac{((m^2_\tau - m^2_{\pi_t}) - 2p^{\perp,2}_{\pi_t})}{2(p^{\perp,2}_{\pi_t} + m^2_{\pi_t})}.p^{\parallel}_{\pi_t} \pm \dfrac{\sqrt{(m^2_\tau - m^2_{\pi_t})^2 - 4m^2_\tau p^{\perp,2}_{\pi_t}}}{2(p^{\perp,2}_{\pi_t} + m^2_{\pi_t})}.E_{\pi_t} \end{cases}$$

- A selection rule has to be build in order to solve the ambiguities.
- Practically energy-momentum conservation at the B decay vertex gives a condition between τ's and K^* :

$$p_{\tau^+_-} = -\frac{\vec{p}^{\perp}_{K*}.\vec{e}_{\tau^+_-}}{1-(\vec{e}_{\tau^+_-}.\vec{e}_B)^2} - p_{\tau^-_+}.\frac{\vec{e}_{\tau^+_-}.\vec{e}_{\tau^-_+} - (\vec{e}_{\tau^+_-}.\vec{e}_B)(\vec{e}_{\tau^-_+}.\vec{e}_B)}{1-(\vec{e}_{\tau^+_-}.\vec{e}_B)^2}$$

- Method validated at MC truth level.

Working points

- PV : 3D normal law including Beam Spot Constraints.
- SV & TV $\rightarrow$ ellipsoidal (decaying particle direction as reference) :
  - longitudinal,
  - transverse.
- Several working points examined (Longitudinal-Transverse configuration denoted as L-T in the following) :
  - 5 µm to 20 µm longitudinal,
  - 1 µm to 8 µm transverse.
- 20-3 (L-T) smearing used as reference in the following.
- Experimental vertexing efficiency is conservatively taken as 80% for the time being [i].

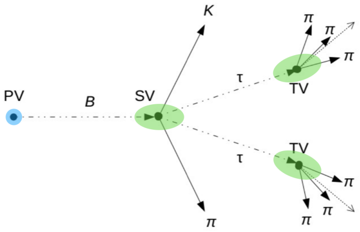

i. Due to the large multiplicity of the decay FCCAnalyses vertexing failed to estimate efficiency by itself.

The considered backgrounds

- The relevant backgrounds are the ones with a similar final state than the signal ($K7\pi$).
- Several possible modes in $b \to c\bar{c}s$ and $b \to c\tau\nu$ transitions[ii] but often not observed to date $\Rightarrow$ guesstimate of the branching fraction from phase space computation and use of analogies.
- Determination of the dominant backgrounds for the measurement by estimating per track efficiencies from 3 already generated backgrounds.

ii. **More details on backgrounds choices in appendix.**

The considered backgrounds

- The relevant backgrounds are the ones with a similar final state than the signal ($K7\pi$).
- Several possible modes in $b \to c\bar{c}s$ and $b \to c\tau\nu$ transitions[ii] but often not observed to date $\Rightarrow$ guesstimate of the branching fraction from phase space computation and use of analogies.
- Determination of the dominant backgrounds for the measurement by estimating per track efficiencies from 3 already generated backgrounds.

Decay	BF (SM/meas.)	Intermediate decay	BF_had	Additional missing particles
Signal : $B^0 \to K^*\tau\tau$	1.30×10^{-7}	$\tau \to \pi\pi\pi\nu$, $K^* \to K\pi$	9.57×10^{-11}	
Backgrounds $b \to c\bar{c}s$:				
$B^0 \to K^{*0}D_sD_s$	5.47×10^{-5}	$D_s \to \tau\nu$	1.14×10^{-10}	2ν
		$D_s \to \tau\nu, \pi\pi\pi\pi^0$	1.28×10^{-10}	ν , π^0
		$D_s \to \pi\pi\pi\pi^0$	1.45×10^{-10}	$2\pi^0$
		$D_s \to \tau\nu, \pi\pi\pi\pi^0\pi^0$	1.08×10^{-9}	ν , $2\pi^0$
		$D_s \to \pi\pi\pi 2\pi^0$	1.02×10^{-8}	$4\pi^0$
$B^0 \to K^{*0}D_sD_s^*$	1.73×10^{-4}	$D_s \to \tau\nu$	3.60×10^{-10}	2ν, γ/π^0
		$D_s \to \pi\pi\pi\pi^0\pi^0$	3.22×10^{-8}	$4\pi^0$, γ/π^0
Backgrounds $b \to c\tau\nu$:				
$B^0 \to K^{*0}D_s\tau\nu$	9.17×10^{-6}	$D_s \to \tau\nu$	3.59×10^{-10}	2ν
$B^0 \to K^{*0}D_s^*\tau\nu$	2.03×10^{-5}	$D_s \to \pi\pi\pi\pi^0\pi^0$	7.51×10^{-9}	ν, γ, $2\pi^0$

ii. **More details on backgrounds choices in appendix.**

Selection

- The B^0 mass has been reconstructed for all our modes.
- Calorimeter PID performances : π^0 detection rate of 80% is assumed in order to reduce the π^0 backgrounds.
- Backgrounds are overwhelming.
- Additional selection is required. We played a Multivariate selection [iii] with XGBoost [9].
- Purity of the signal (S/B) evaluated on the $[5.2, 5.6]\text{GeV}/c^2$ window to quantify the improvement at each selection step.

	Signal purity
No selection	0.11
Preselection	0.44
Final selection	3.04

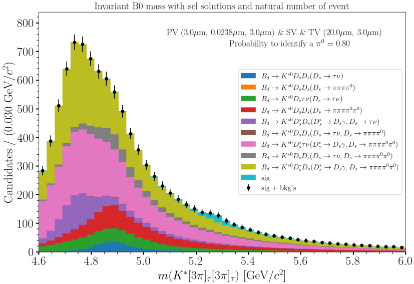

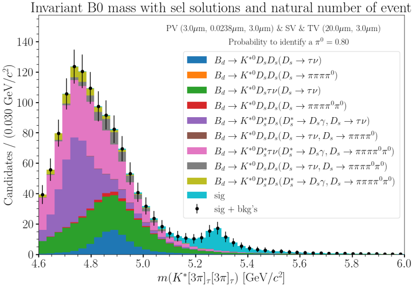

iii. **More details in appendix.**

IDEA working points

- In addition of the fastly emulated vertexing performances : use of a state of the art detector working point.
- The IDEA vertexing resolutions have been fitted [iv] from signal events for each vertices.
- Emulation of the IDEA vertexing performances from a smearing that follow the fitted resolutions.

Additional working points

- The SmearObjects.SmearedTracks tools allows to use IDEA vertexing with tracks improvements.
- 4 various IDEA working points examined with better Ω (momentum measurement) or IP resolutions.

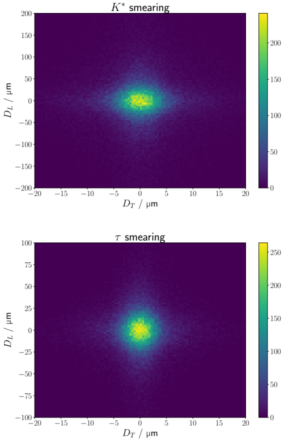

Example of 2D smearing used to emulate the SV (top) and TV (bottom) IDEA resolutions.

iv. More details in appendix.

Determination of the measurement precision

- Same selection applied to all vertex resolution emulations.
- Unbinned ML fit of the data with :
  - signal $\rightarrow$ double CB + a Gaussian,
  - background $\rightarrow$ two decreasing exponential.
- Fitting scheme :
  1. fit of the simulated signal
  2. fit of the signal and background rescaled w.r.t. their yields
- Extraction of the signal yield N and the associated error σ_N.
- Precision of the BF measurement of $B^0 \rightarrow K^{*0}\tau\tau$ given by σ_N/N [v].

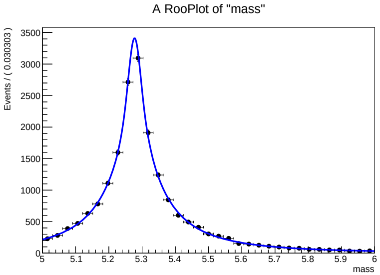

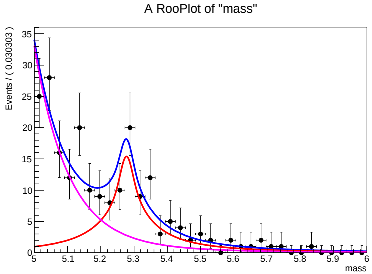

v. **Precision plot with the fastly emulated points in appendix.**

Precision of the measurement

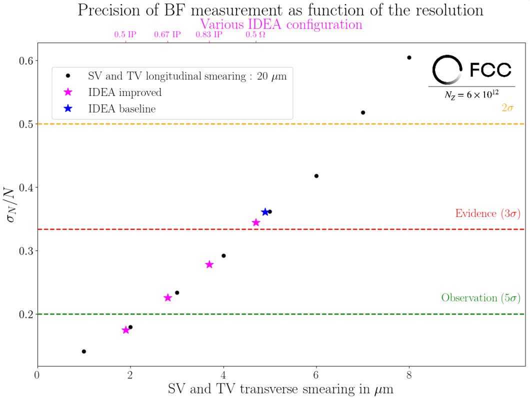

Emulation of the vertex resolution performances in order to look for the feasibility of the search of $B^0 \to K^{*0}\tau\tau$ at FCC-*ee* :

- IDEA baseline close to the evidence,
- IP measurements improvement could helps a lot $\Rightarrow$ but what does it mean in term of detector ?

How to practically improve IP resolutions

- Samples with improved detector in term of single hit resolution (from 3 µm to 2 µm for the barrel layers) and/or material budget in the vertex detector layers (-50%) have been simulated.
- **Idea** : build mapping between SmearedTracks and regular detectors improvements from d_0 resolutions fits [vi] with :

$$\sigma_{d_0} = \frac{a(\sqrt{x/X_0})}{p_T} + b(\text{geometry}).$$

- Fail : complicate to put in relation SmeardTracks improvements with detector improvements.
- The single hit resolution improvement is, as expected, linearly correlated to the offset of the resolution.
- The material budget reduction doesn't match the expected $\sqrt{x/X_0}$ slope improvement ? → to be investigated further
- Best thing to do now : emulate these new points.

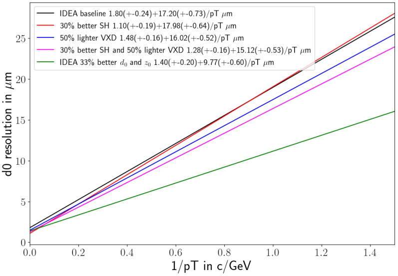

vi. Detailed equation in appendix.

Results

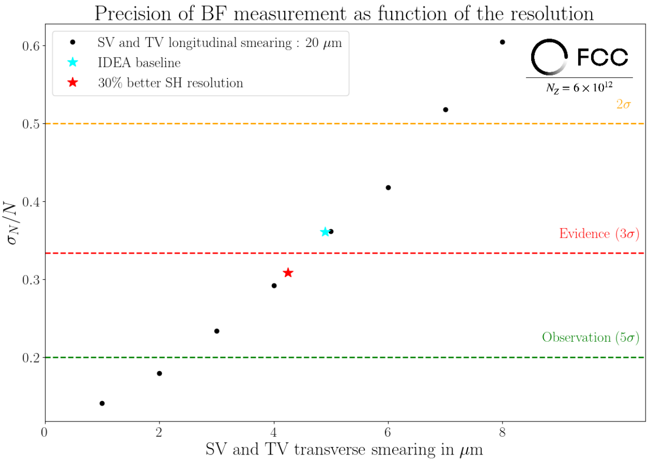

The 30 % single hit resolution improvement allow to reach the 3σ threshold.

Results

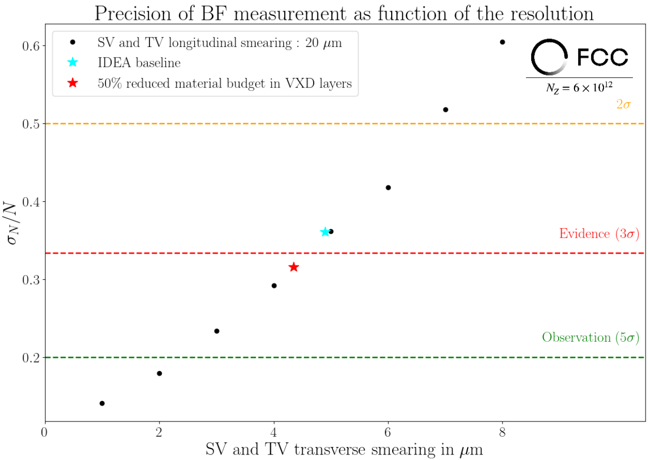

The 50 % reduced material budget in vertex detector has a bit less impact.

Results

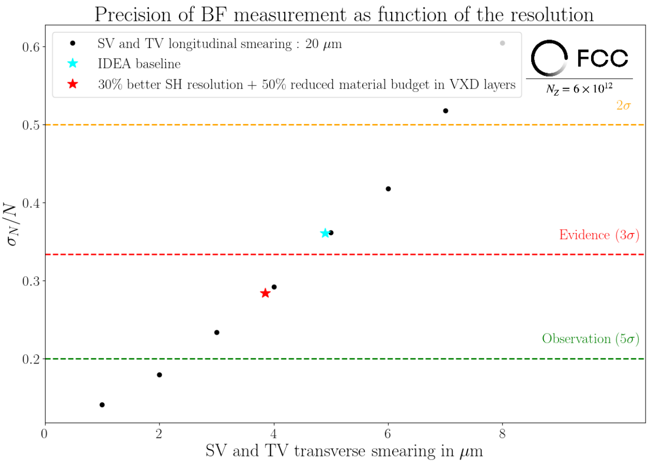

The combination of the two improvements reach only 3.5σ.

Conclusion

Last words

- Analysis aimed at assessing the required vertexing performances to measure $B^0 \to K^{*0}\tau\tau$ from the two $\tau \to 3\pi$ self-contained method only.
- Very demanding even for FCC ...
- But this work has been done under the SM hypothesis $\Rightarrow$ even if not SM there is a lot to win by improving the detector precision.

Conclusion

Last words

- Analysis aimed at assessing the required vertexing performances to measure $B^0 \to K^{*0}\tau\tau$ from the two $\tau \to 3\pi$ self-contained method only.
- Very demanding even for FCC ...
- But this work has been done under the SM hypothesis $\Rightarrow$ even if not SM there is a lot to win by improving the detector precision.

Term of the analysis

- The emulation of the vertexing performance for the "detector like working point" is the best we can do now.
- To close the analysis, we will try to play the full reconstruction of these points from the available tools, to access properly the vertexing efficiency and to challenge the emulations.

Conclusion

Last words

- Analysis aimed at assessing the required vertexing performances to measure $B^0 \to K^{*0}\tau\tau$ from the two $\tau \to 3\pi$ self-contained method only.
- Very demanding even for FCC ...
- But this work has been done under the SM hypothesis $\Rightarrow$ even if not SM there is a lot to win by improving the detector precision.

Term of the analysis

- The emulation of the vertexing performance for the "detector like working point" is the best we can do now.
- To close the analysis, we will try to play the full reconstruction of these points from the available tools, to access properly the vertexing efficiency and to challenge the emulations.

Thanks !

Neutrinos reconstruction method

To fully reconstruct the kinematics of the decay (B invariant-mass observable for instance) we need :

- Momentum of all final particles including not detected neutrinos.
- The decay lengths (6 constraints) together with the tau mass (2 constraints) can be used to determine the missing coordinates (6 degrees of freedom).
- We use energy-momentum conservation at tertiary (or τ decay) vertex with respect to τ direction [vii].

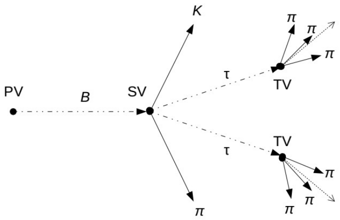

The dotted lines represent the non-reconstructed particles. The plain lines are the particles that can be reconstructed in the detector.

$$\begin{cases} p_{\nu_\tau}^{\perp} = -p_{\pi_t}^{\perp} \\ p_{\nu_\tau}^{\parallel} = \dfrac{((m_\tau^2 - m_{\pi_t}^2) - 2p_{\pi_t}^{\perp,2})}{2(p_{\pi_t}^{\perp,2} + m_{\pi_t}^2)} . p_{\pi_t}^{\parallel} \pm \dfrac{\sqrt{(m_\tau^2 - m_{\pi_t}^2)^2 - 4m_\tau^2 p_{\pi_t}^{\perp,2}}}{2(p_{\pi_t}^{\perp,2} + m_{\pi_t}^2)} . E_{\pi_t} \end{cases}$$

vii. Another way to do this computation is given by [10].

Selection rule

There is a quadratic ambiguity on each neutrino momentum !

$\rightarrow$ The ambiguities propagate to τ and B reconstructions

$\rightarrow$ 4 possibilities by taking all +/- combination for the two neutrinos

$\Rightarrow$ A selection rule is needed to choose the right possibility

$\longrightarrow$ From the energy-momentum conservation at the B decay vertex, we have a condition between the 2 taus and the K^* with respect to the B direction :

$$p_{\tau^+_-} = -\frac{\vec{p}^{\perp}_{K*}.\vec{e}_{\tau^+_-}}{1-(\vec{e}_{\tau^+_-}.\vec{e}_B)^2} - p_{\tau^-_+}.\frac{\vec{e}_{\tau^+_-}.\vec{e}_{\tau^-_+} - (\vec{e}_{\tau^+_-}.\vec{e}_B)(\vec{e}_{\tau^-_+}.\vec{e}_B)}{1-(\vec{e}_{\tau^+_-}.\vec{e}_B)^2}$$

Expected number of events

The knowledge of the reconstruction efficiency allows us to compute the expected number of B^0 decays fully reconstructed at FCC-*ee* :

$$\mathcal{N}_{K^*\tau\tau\to K7\pi2\nu} = \mathcal{N}_Z.BR(Z\to b\bar{b}).2f_d.BR(K^*\tau\tau).BR(\tau\to\pi\pi\pi\nu)^2.BR(K^*\to K\pi).\epsilon_{reco}.\epsilon_{vertex}$$

Where :

- $\mathcal{N}_Z = 6\times10^{12}$ the expected number of Z produced,
- $BR(Z\to b\bar{b}) = 0.1512 \pm 0.0005$,
- $f_d = 0.407 \pm 0.007$ the hadronisation term,
- $BR(K^*\tau\tau) = 1.30\times10^{-7} \pm 10\%$ the SM predicted branching fraction,
- $BR(\tau\to\pi\pi\pi\nu) = 0.0931 \pm 0.0005$,
- $BR(K^*\to K\pi) = 0.69$,
- $\epsilon_{reco} = 0.3840 \pm 0.0007$ for a smearing $3\,\mu m - 20\,\mu m$,
- $\epsilon_{vertex} = 0.8$,

$$\Rightarrow \mathcal{N}_{K^*\tau\tau\to K7\pi2\nu} \approx 176 \pm 18$$

Some words about guesstimation of the BF for unseen modes

- $B^0 \to K^{*0} D_s D_s$ from analogy game and form factors / phase space corrections :

$$BF(B^0 \to K^{*0} D_s D_s) = BF(B^+ \to K^+ D_s^+ D_s^-) \times C_{\rm FF} \times C_{\rm PS}$$

where $B^+ \to K^+ D_s D_s$ (recently measured by LHCb) has the same quark content than $B^0 \to K^{*0} D_s D_s$ but the spectator quark.

- Form factor correction K vs K^* from :

$$C_{\rm FF} = \frac{\rm FF_{K^*}}{\rm FF_K} = \frac{BF(B^+ \to D^0 K^{*+})}{BF(B^+ \to D^0 K^+)}.$$

- Phase space K vs K^*, from PS computed numerically (three body decay hypothesis used conservatively) :

$$C_{\rm PS} = \frac{PS(B^+ \to K^{*+} D_s^+ D_s^-)}{PS(B^+ \to K^+ D_s^+ D_s^-)}.$$

- $B^0 \to K^{*0} D_s^* D_s$ and $B^0 \to K^{*0} D_s^* D_s^*$ w.r.t. $B^0 \to K^{*0} D_s D_s$ from $B_s^0 \to D_s^{(*)} D_s^{(*)}$ hierarchy.

Some words about guesstimation of the BF for unseen modes

- $B^0 \to K^{*0} D_s^{(*)} \tau\nu$ from analogy via phase space computation [10] :

$$BF(B^0 \to K^{*0} D_s^{(*)} \tau\nu) = BF(B^+ \to K D_s^{(*)} \ell\nu) \times \frac{PS(B^0 \to K^{*0} D_s^{(*)} \tau\nu)}{PS(B^+ \to K D_s^{(*)} \ell\nu)}$$

  where PS denotes the Phase Space computed numerricaly (three body decay hypothesis used conservatively) and $B^+ \to K D_s^{(*)} \ell\nu$ is a reference mode with a known BF.

- $B^0 \to K^{*0} D_s \tau\nu$ and $B^0 \to K^{*0} D_s^* \tau\nu$ w.r.t $B^0 \to K^{*0} D_s^{(*)} \tau\nu$ from $B^0 \to D^{(*)} \ell\nu$ hierarchy.
- $B_s^0 \to K^{*0} D^{(*)} \tau\nu$ from analogy via phase space computation [10] :

$$BF(B_s^0 \to K^{*0} D^{(*)} \tau\nu) = BF(B_s^0 \to D_{s1} \mu\nu) \times \frac{PS(B_s^0 \to K^{*0} D^{(*)} \tau\nu)}{PS(B_s^0 \to D_{s1} \mu\nu)}$$

  where PS denotes the Phase Space computed numerricaly (three body decay hypothesis used conservatively) and $B_s^0 \to D_{s1} \mu\nu$ is a reference mode with a known BF.

- $B_s^0 \to K^{*0} D \tau\nu$ and $B_s^0 \to K^{*0} D^* \tau\nu$ w.r.t. $B_s^0 \to K^{*0} D^{(*)} \tau\nu$ from $B^0 \to D^{(*)} \ell\nu$ hierarchy.

Extended background table

Decay	BF (SM/meas.)	Intermediate decay	BF_had	Additional missing particles
Signal : $B^0 \to K^* \tau\tau$	1.30×10^{-7}	$\tau \to \pi\pi\pi\nu$, $K^* \to K\pi$	9.57×10^{-11}	
Backgrounds $b \to c\bar{c}s$:				
$B^0 \to K^{*0} D_s D_s$	5.47×10^{-5}	$D_s \to \tau\nu$	1.14×10^{-10}	2ν
		$D_s \to \tau\nu, \pi\pi\pi\pi^0$ viii	1.28×10^{-10}	ν , π^0
		$D_s \to \pi\pi\pi\pi^0$ viii	1.45×10^{-10}	$2\pi^0$
		$D_s \to \tau\nu, \pi\pi\pi\pi^0\pi^0$	1.08×10^{-9}	ν , $2\pi^0$
		$D_s \to \pi\pi\pi 2\pi^0$ viii	1.02×10^{-8}	$4\pi^0$
$B^0 \to K^{*0} D_s D_s^*$	1.73×10^{-4}	$D_s \to \tau\nu$	3.60×10^{-10}	2ν, γ/π^0
		$D_s \to \tau\nu, \pi\pi\pi\pi^0$	4.06×10^{-10}	ν , π^0, γ/π^0
		$D_s \to \pi\pi\pi\pi^0$	4.57×10^{-10}	$2\pi^0$, γ/π^0
		$D_s \to \pi\pi\pi\pi^0\pi^0$	3.22×10^{-8}	$4\pi^0$, γ/π^0
$B^0 \to K^{*0} D_s^* D_s^*$	1.79×10^{-4}	$D_s \to \tau\nu$	3.73×10^{-10}	2ν, $2\gamma/\pi^0$
		$D_s \to \tau\nu, \pi\pi\pi\pi^0$	4.20×10^{-10}	ν , π^0, $2\gamma/\pi^0$
		$D_s \to \pi\pi\pi\pi^0$	4.73×10^{-10}	$2\pi^0$, $2\gamma/\pi^0$
Backgrounds $b \to c\tau\nu$:				
$B_s \to K^{*0} D\tau\nu$	7.27×10^{-5}	$D \to \pi\pi\pi\pi^0$	1.65×10^{-9}	ν, π^0
$B_s \to K^{*0} D^*\tau\nu$	2.03×10^{-4}	$D^* \to D^0\pi, D\pi^0$		
		$D \to \pi\pi\pi\pi^0$	1.12×10^{-9}	ν, $2\pi^0$
		$D^0 \to 2\pi 2\pi\pi^0$	8.98×10^{-10}	ν, $2\pi^0$, $2\pi^\pm$
$B^0 \to K^{*0} D_s\tau\nu$	9.17×10^{-6}	$D_s \to \tau\nu$	3.59×10^{-10}	2ν
		$D_s \to \pi\pi\pi\pi^0$	4.05×10^{-10}	ν, π^0
$B^0 \to K^{*0} D_s^*\tau\nu$	2.03×10^{-5}	$D_s \to \tau\nu$	8.07×10^{-10}	2ν, γ/π^0
		$D_s \to \pi\pi\pi\pi^0$	9.09×10^{-10}	ν, π^0, γ/π^0
		$D_s \to \pi\pi\pi\pi^0\pi^0$	7.51×10^{-9}	ν, γ, $2\pi^0$

viii. $D_s \to 3\pi n\pi^0$ modes involves η/ω intermediate states.

Update of the $D_s \to \pi\pi\pi n\pi^0$ simulation

Better simulations for $D_s \to \pi\pi\pi n\pi^0$

- Previously this decay has been generated in the Phase Space $\to$ a more accurate simulation of the decay is needed $\Rightarrow$ new samples which include η/ω (saturating the inclusive BF) intermediate states are in order.
- Replacement of the previous samples.
- $B^0 \to K^{*0} D_s D_s (D_s \to \pi\pi\pi\pi^0)$ is now $B^0 \to K^{*0} D_s D_s$ where $D_s \to \eta/\omega\pi$ and $\eta/\omega \to \pi\pi\pi^0$.
- $B^0 \to K^{*0} D_s D_s (D_s \to \pi\pi\pi\pi^0\pi^0)$ is now $B^0 \to K^{*0} D_s D_s$ where $D_s \to \eta/\omega\pi\pi^0$ and $\eta/\omega \to \pi\pi\pi^0$.

Distribution of π^0 momentum from $D_s \to 3\pi2\pi^0$

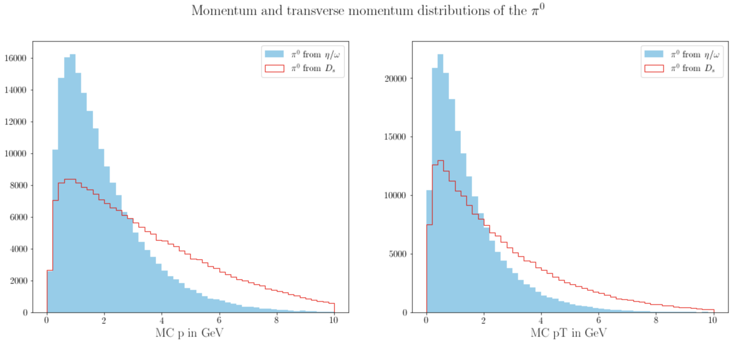

Distribution of π^0 momentum from $D_s \to 3\pi2\pi^0$.

Some word about the choice of background to consider

- $B^0 \to K^{*0} D_s D_s$ with the two D_s deacying as $D_s \to \tau\nu$, $D_s \to \pi\pi\pi\pi^0$ and $D_s \to \pi\pi\pi\pi^0\pi^0$ already generated.
- $B^0 \to K^{*0} D_s^* D_s$ with the two D_s deacying as $D_s \to \tau\nu$ already generated.
- $B^0 \to K^{*0} D_s D_s$ with both $D_s \to \tau\nu$ and $D_s \to \pi\pi\pi\pi^0$ already generated.
- Construction of a "per track" efficiency by taking the square root of the reconstruction efficiency of the four first modes $\Rightarrow \epsilon(D_s \to \tau\nu)$, $\epsilon(D_s^* \to \tau\nu)$, $\epsilon(D_s \to \pi\pi\pi\pi^0)$ and $\epsilon(D_s \to \pi\pi\pi\pi^0\pi^0)$.
- Cross check : $\epsilon(D_s \to \tau\nu) \times \epsilon(D_s \to \pi\pi\pi\pi^0) \simeq \epsilon(B^0 \to K^{*0} D_s D_s, D_s \to \tau\nu, D_s \to \pi\pi\pi\pi^0)$.
- Construction of an $\epsilon(*) = \epsilon(D_s^* \to \tau\nu)/\epsilon(D_s \to \tau\nu)$.
- Computation of an estimated efficiency for the possible background from these per track efficiencies.
- Ranking of the backgrounds via $BF \times \epsilon$.
- Choice of the biggest one for each type of specific topology.

Reconstruction efficiency

Mode	Total reconstruction efficiency (%)
Signal	38.40 ± 0.07
$B^0 \to K^{*0} D_s D_s$, $D_s \to \tau\nu$	47.49 ± 0.04
$B^0 \to K^{*0} D_s D_s$, $D_s \to 3\pi\pi^0$	2.190 ± 0.002
$B^0 \to K^{*0} D_s D_s$, $D_s \to 3\pi 2\pi^0$	56.30 ± 0.05
$B^0 \to K^{*0} D_s D_s$, $D_s \to \tau\nu/3\pi\pi^0$	10.14 ± 0.01
$B^0 \to K^{*0} D_s D_s$, $D_s \to \tau\nu/3\pi 2\pi^0$	51.64 ± 0.04
$B^0 \to K^{*0} D_s^* D_s$, $D_s \to \tau\nu$	48.27 ± 0.04
$B^0 \to K^{*0} D_s^* D_s$, $D_s \to 3\pi 2\pi^0$	57.30 ± 0.04
$B^0 \to K^{*0} D_s \tau\nu$, $D_s \to \tau\nu$	42.85 ± 0.04
$B^0 \to K^{*0} D_s^* \tau\nu$, $D_s \to 3\pi 2\pi^0$	47.26 ± 0.04

Summary table of the total reconstruction (including the B^0 candidate building and neutrino reconstruction) efficiency as function of the mode for the reference vertexing performances working point.

Landscape without selection

- The B^0 mass has been reconstructed for all our modes.
- Calorimeter PID performances : π^0 detection rate of 80% is assumed in order to reduce the π^0 backgrounds.
- Backgrounds are overwhelming.
- Additional selection is required. We played a Multivariate selection (XGBoost [9]).

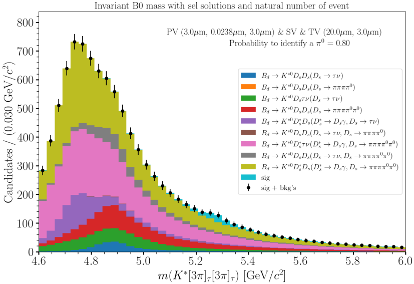

Signal purity [ix]	0.11

ix. Signal purity is defined as S/B and evaluated on the [5.2, 5.6]GeV/c^2 window.

Preselection

- Several kinematics variables has been save for each events (like momentum or intermediate mass).
- Among them several discriminatives variables have been found[×].
- The preselection has been built with these variables.
- The plot displays the result after preselection → the picture show a first improvement.
- The MVA can be trained against the backgrounds on the [5,5.6] GeV mass window.

Variable	Cut
$m^2_{2\pi\,min}$ & $m^2_{2\pi\,max}$	< 0.3 & < 0.5 GeV
p_{K^*}	$<$ 1GeV
$p_{3\pi}$	$<$ 1GeV
$p_{\pi\,max}$	$<$ 0.25GeV
$p_{\pi\,min}$	$<$ 0.2GeV
FD_B	$<$ 0.3mm
FD_τ	$>$ 4mm
$m_{3\pi}$	$<$ 0.750GeV
$m_{2\pi\,max}$	$<$ 0.5GeV
$m_{2\pi\,min}$	$>$ 1GeV

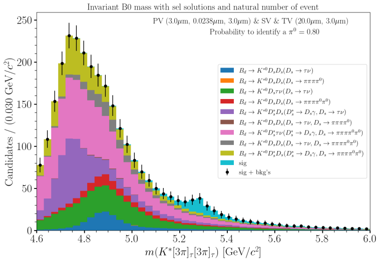

Signal purity	0.44

[×] Example of discriminative variables in appendix

MVA

- Training dataset generated with signal and the collection of available backgrounds.
- The backgrounds are considered in natural proportion (after the preselection).
- 50/50 split train/validation.
- Previous variables are given as inputs as well as the reconstructed p_τ of each τ candidate.
- XGB parameters optimised on AUC.
- Overtraining plot in order to check the validity of the training $\rightarrow$ OK.
- Use of the MVA [xi] to perform the selection (cut at 0.5 on the BDT output).

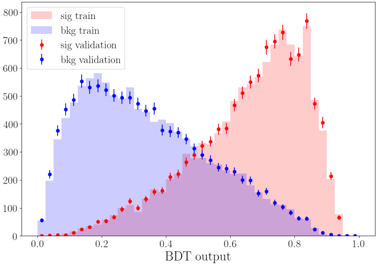

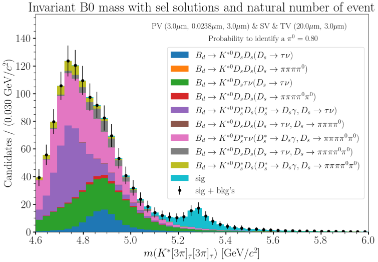

Signal purity	3.04

xi. **Feature importance plot in appendix.**

Reconstructed p_{tau} distribution signal vs backgrounds $20-3$ configuration

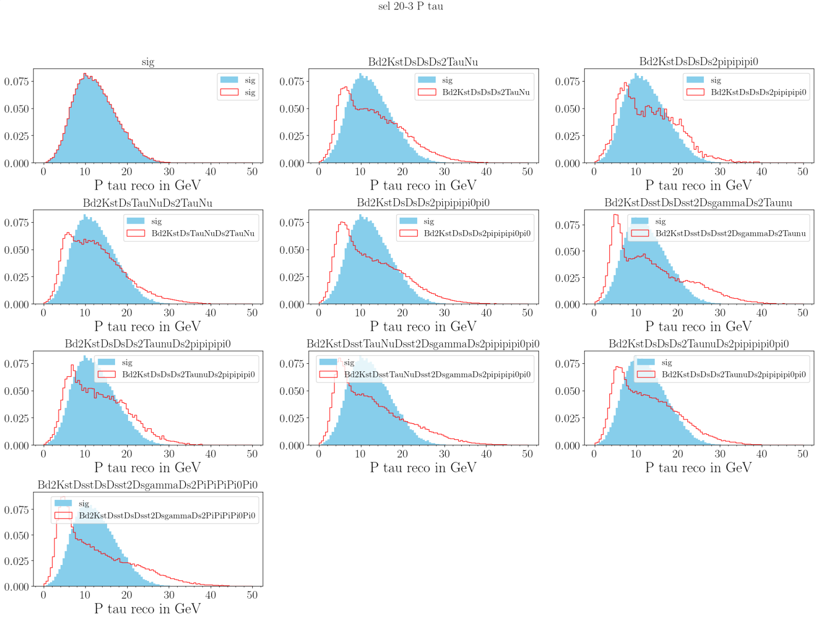

FD_τ distribution signal vs backgrounds 20 − 3 configuration

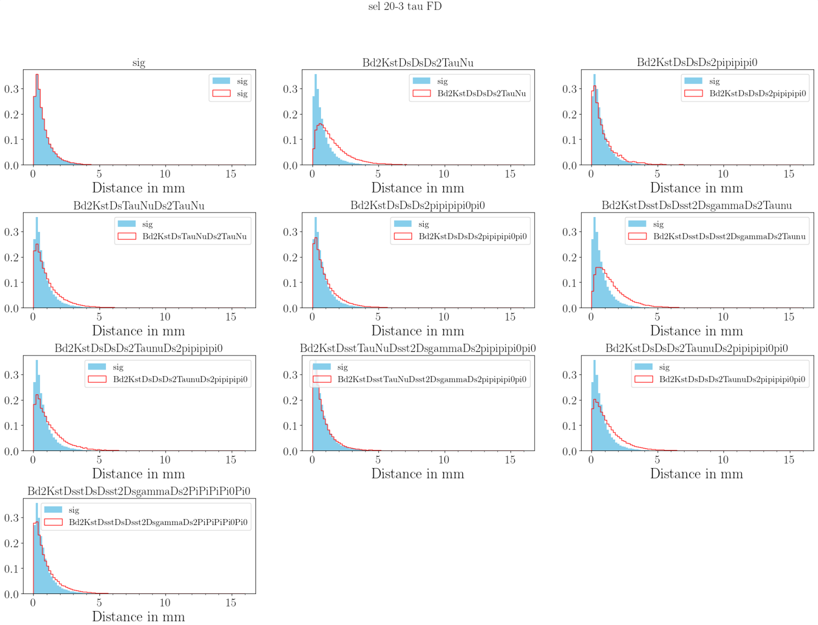

Dalitz plane ($m^2_{\pi_{max}}$, $m^2_{\pi_{min}}$) signal and backgrounds 20 − 3 configuration

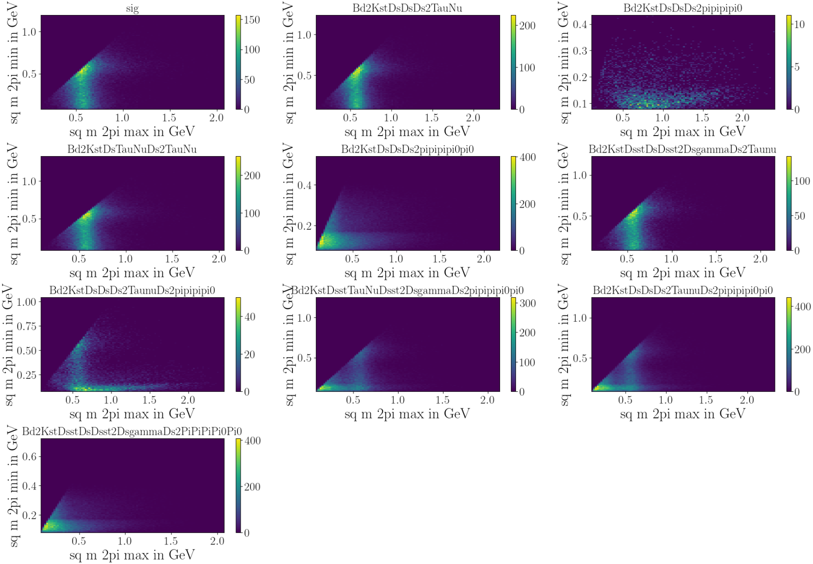

XGB features importances

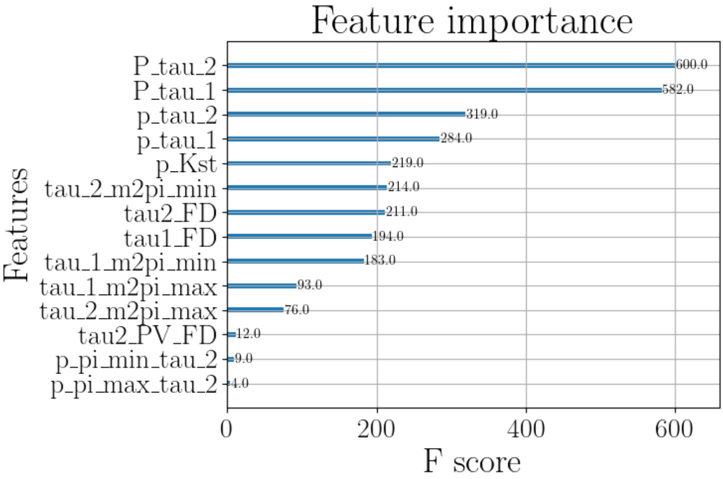

Precision of the measurement with other longitudinal resolutions.

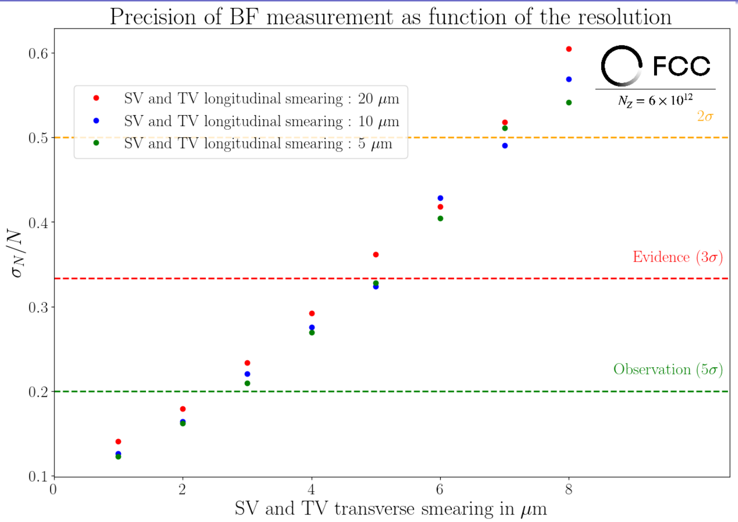

Precision on the BF measurement as function of the vertex resolution with 3 longitudinal configurations. Observed hierarchy issue comes from the interplay between the smearing of the vertexing and the fit model.

The IDEA working point : primary vertex resolution

- Resolutions determined from 10^6 signal events.
- Reconstructed PV position fitted from reconstructed tracks with the FCCAnalyses VertexFitterSimple tools (Beam Spot Constraints set at $(4.5, 20e^{-3}, 300)\mu\text{m}$).
- Displacement of the reconstructed PV w.r.t. the MC truth PV is build in cartesian coordinates.
- The IDEA resolution is determined for each coordinate by a fit of the displacement :
    - double gaussian model on (x,z) [xii],
    - simple gaussian model on y.
- Resolutions $\mathcal{O}(3\,\mu\text{m})$ for (x,z).
- Resolution $\mathcal{O}(20\,\text{nm})$ for y.

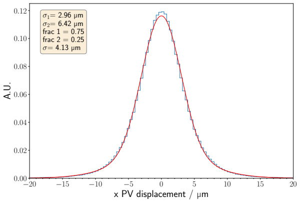

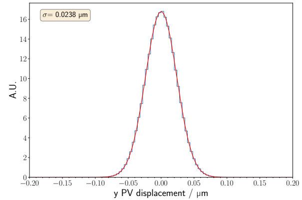

PV displacement and fit of the resolution for x (top) and y (bottom).

xii. In appendix.

The IDEA working point : secondary and tertiary vertices resolutions

- Reconstructed SV ($K^{*0} \to K\pi$) and TV ($\tau \to 3\pi$) positions fitted from MC matched reconstructed tracks via FCCAnalyses VertexFitterSimple tools.
- Displacement of the reconstructed SV and TV w.r.t. to the MC truth projected on decay plan (L-T).
- Signed decomposition of the transverse displacement determined from two orthogonal directions pick-up randomly via a circle parameterized in the transverse plan itself.
- The IDEA resolution is determined for each coordinate by a fit of the displacement with a triple gaussian model.

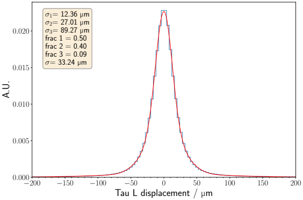

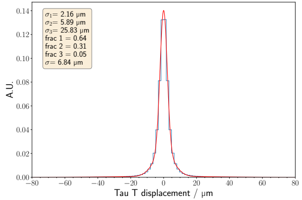

TV displacement and fit of the resolution for L (top) and T (bottom) directions.

The IDEA working point : emulation

- Emulation of the PV resolutions with 3D-gaussian smearing that follow the combined σ of the fits among each axis.
- SV and TV smearing via the IDEA fitted resolutions.
- Smearing emulated on each direction via accept/reject algorithms.

Additional working points

- The SmearObjects.SmearedTracks tools allows to use IDEA vertexing with brutal tracks improvements.
- 4 various IDEA working points examined with better Ω (momentum) or IP resolutions.

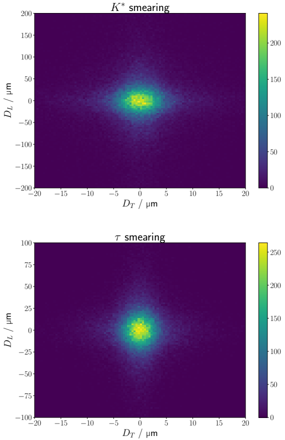

Example of 2D smearing used to emulate the SV (top) and TV (bottom) IDEA resolutions.

Other IDEA resolution plots

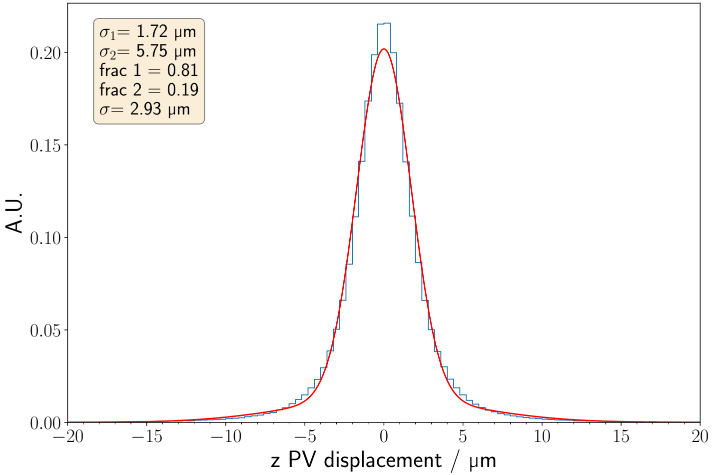

PV displacement and fit of the resolution for z

Other IDEA resolution plots

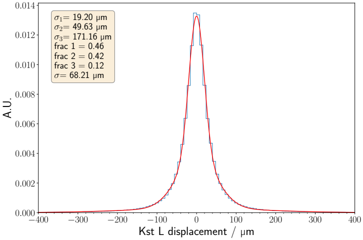

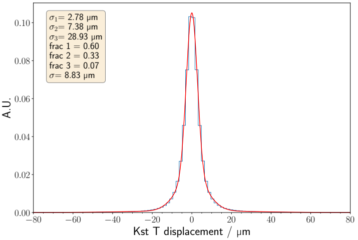

SV displacement and fit of the resolution for L (top) and T (bottom).

More detailed about IP resolution

Complete equation :

$$\sigma_{\mathrm{d}_0} \simeq \sqrt{\frac{r_2^2\sigma_1^2 + r_1^2\sigma_2^2}{(r_2 - r_1)^2}} \oplus \frac{r}{p_T \sin^{1/2}\theta} 13.6\,\mathrm{MeV}\sqrt{\frac{x}{X_0}},$$

where the first term is link to detector resolution and the second to multiple scattering. $r_{1(2)}$ is the distance between the first (second) hit of the track and the PV, $\sigma_{1(2)}$ is the resolution on the first (second) hit of the track. r is the distance between the PV and the contact points of the track with the vertex detector layer, p_T is the transverse momentum of the track, θ is the polar angle of the track, x is the thickness and X_0 is the radiation length.

Paul Langacker.
The physics of heavy z' gauge bosons.
Reviews of Modern Physics, 81(3) :1199, 2009.

I Dorsner, S Fajfer, A Greljo, JF Kamenik, and N Kosnik.
Physics of leptoquarks in precision experiments and at particle colliders.
Physics Reports, 641 :1–68, 2016.

JF Kamenik, S Monteil, A Semkiv, and L Vale Silva.
Lepton polarization asymmetries in rare semi-tauonic $b \to s$ b→ s exclusive decays at fcc-ee.
The European Physical Journal C, 77(10) :1–19, 2017.

BABAR Collaboration et al.
Search for b+-> k+ tau (+) tau (-) at the babar experiment.
Physical Review Letters, 2017, vol. 118, num. 3, p. 031802, 2017.

- Torbjörn Sjöstrand, Stefan Ask, Jesper R Christiansen, Richard Corke, Nishita Desai, Philip Ilten, Stephen Mrenna, Stefan Prestel, Christine O Rasmussen, and Peter Z Skands.
  An introduction to pythia 8.2.
  Computer physics communications, 191 :159–177, 2015.
- Anders Ryd, David Lange, Natalia Kuznetsova, Sophie Versille, Marcello Rotondo, DP Kirkby, FK Wuerthwein, and A Ishikawa.
  Evtgen : a monte carlo generator for b-physics.
  BAD, 522 :v6, 2005.
- J De Favereau, Christophe Delaere, Pavel Demin, Andrea Giammanco, Vincent Lemaitre, Alexandre Mertens, Michele Selvaggi, Delphes 3 Collaboration, et al.
  Delphes 3 : a modular framework for fast simulation of a generic collider experiment.
  Journal of High Energy Physics, 2014(2) :57, 2014.

CERN.
2nd fcc-france workshop, jan 20-21, 2021.
https:...Physics.pdf.

Tianqi Chen and Carlos Guestrin.
Xgboost : A scalable tree boosting system.
In *Proceedings of the 22nd acm sigkdd international conference on knowledge discovery and data mining*, pages 785–794, 2016.

Lingfeng Li and Tao Liu.
$b \to s\tau + \tau$- physics at future z factories.
Journal of High Energy Physics, 2021(6) :1–31, 2021.